

Spectroscopic (FT-IR, FT-Raman, NMR) investigations, MEP and Magnetic Susceptibility of 2,3-diphenyl-5-(thiophen-2-ylmethylidene)-2,5-dihydro-1,2,4-triazin-6(1H)-one

M. Murali¹, V. Balachandran² and B. Narayana³

¹Department of Physics, CARE Group of Institutions, Tiruchirappalli, India – 620 009.

²Centre for Research-Department of Physics, Arignar Anna Govt. Arts College, Musiri, Tiruchirappalli 621211, India.

³Department of Studies in Chemistry, Mangalore University, Mangalagangothri 574 199, India.

ARTICLE INFO

Article history:

Received: 26 June 2017;

Received in revised form:

27 July 2017;

Accepted: 5 August 2017;

Keywords

Thiophene,
FTIR,
FT Raman,
Fukui function,
MEP,
2,3-diphenyl-5-(thiophen-2-ylmethylidene)-2,5-dihydro-1,2,4-triazin-6(1H)-one,
Magnetic susceptibility.

ABSTRACT

In the present work, a combined experimental and theoretical study on ground state molecular structure, spectroscopic and nonlinear optical properties of the thiophene derivative 2,3-diphenyl-5-(thiophen-2-ylmethylidene)-2,5-dihydro-1,2,4-triazin-6(1H)-one is reported. The entire quantum chemical calculations and optimized structural parameters like bond lengths and bond angles, vibrational frequencies and optimized geometry have performed at DFT/B3LYP method with cc-pVDZ and cc-pVTZ basis sets using the Gaussian 09W program package. The calculated results show that the optimized geometry parameters, the theoretical vibrational frequencies and chemical shift values show good agreement with experimental values. The FTIR and FT Raman spectra of the title compound have been recorded in the regions 4000 – 400 cm⁻¹ and 3500 – 100 cm⁻¹, respectively. The calculated harmonic vibrational frequencies have been compared with experimental FT-IR and FT-Raman spectra. The observed and calculated frequencies are found to be in good agreement. In addition, Mulliken atomic charges, local reactivity descriptors such as local softness (sk), Fukui function (fk), global electrophilicity and nucleophilicity of the title compound were calculated and discussed. Besides HOMO–LUMO energy gap and molecular electrostatic potential map were performed. ¹H and ¹³C NMR isotropic chemical shifts are evaluated experimentally. Magnetic susceptibility has been determined for various range of temperature.

© 2017 Elixir All rights reserved.

1. Introduction

Thiophene is one of the most studied heterocycles: it is easy to process, chemically stable, and its synthetic applications have been a constant matter of investigation for many years [1]. Thiophene belongs to a class of heterocyclic compounds containing a five-membered ring made up of one sulphur as heteroatom with the formula C₄H₄S[2]. In medicinal chemistry, thiophene derivatives have been very well known for their therapeutic applications. The normal thiophenes are stable liquids which is very similar to the benzene compounds in the character like boiling point and in smell[3]. Thiophene has a structure that is analogous to structure of pyrrole, and due to pie electron cloud, it behaves like extremely reactive benzene derivative.[4] In most cases, the 2nd and 5th position of thiophene are used for the polymerization[5]. The modification of the molecules for special electronic properties is operated on the 3rd and 4th - positions[6]. Thiophenes are part of many organic compounds[7] having vast applications in the field of electronics and optoelectronics, medicine and materials [8-10]. The remarkable pharmacological efficiency of the compounds containing a thiophene ring in their structure is known for their antidepressant, anticonvulsant, antihistaminic, anaesthetic, antipuritic, analgesic action [11].

Thiophene and its derivatives exhibit diverse biological properties such as nemotocidal[12], insecticidal[13], antibacterial, antifungal, antiviral and antioxidant activity [14].

Density functional theory (DFT) approaches, especially those using hybrid functional, have evolved to a powerful and very reliable tool, being routinely used for the determination of various molecular properties [15]. B3LYP functional has been shown to provide an excellent compromise between accuracy and computational spectra for molecules of large and medium size [16, 17]. The aim of the present study is to give a complete description of the molecular geometry and molecular vibrations of the title molecule. For that purpose, quantum chemical computations were carried out on title molecule using DFT. The calculated HOMO (Highly occupied molecular orbital's) and LUMO (Lowest Unoccupied molecular orbital's) energies show that charge transfer occurs in the title molecule. DFT calculations are characterised to give very good vibrational frequencies of organic compounds if the calculated frequencies, are scaled to indemnify correlation, for basis set deficits and for not simple harmonic [18-20].

Tele:

E-mail address: brsbala@rediffmail.com

© 2017 Elixir All rights reserved

2. Experimental details

The Fourier transform infrared (FT-IR) spectrum of the sample was recorded at room temperature in the region 4000–400 cm^{-1} using Perkin–Elmer spectrum RX1 spectrophotometer equipped with composition of the pellet. The signals were collected for 100 scans with a scan interval of 1cm^{-1} and at optical resolution of 0.4cm^{-1} . The Fourier transform Raman (FT-Raman) BRUKER-RFS 27 spectrometer was used for the Raman spectral measurements at room temperature. The spectrometer consisted of a quartz beam splitter and a high sensitive germanium diode detector cooled to the liquid nitrogen temperature. The sample was packed in a glass tube of about 5 mm diameter and excited in the 180° geometry with 1064 nm laser line at 100mW power from a diode pumped air cooled Nd:YAG laser as an excitation wavelength in the region 4000–100 cm^{-1} . Nuclear magnetic resonance (NMR) spectra were recorded on a Bruker 300 AVANCE spectrometer at 300 MHz for ^1H and 75 MHz for ^{13}C in CDCl_3 solutions containing 0.03 vol.% TMS as internal standard.

3. Computational details

All DFT calculations of the title compound were carried out using Gaussian 09 program package using default thresholds and parameters [21]. The ground state structural geometries were fully optimized at the B3LYP method along with the standard cc-pVDZ and cc-pVTZ basis sets.

In the DFT calculations the Lee, Yang and Parr correlation functional is used together with Becke's three parameters exchange functional B3LYP. The geometry optimization was performed at the B3LYP density functional theory with the same basis set [22, 23]. Harmonic vibrational frequencies were computed at the same level of theory. Structural analysis of the molecules has been executed to have an idea about the lowest energy structures of the category [24]. The molecular geometry has not been limited and all the calculations (vibrational wavenumbers, optimized geometric parameters and other molecular properties) have been performed using the GaussView molecular visualization program and the Gaussian 09W program package. The chemical reactivity behaviour of the compound was predicted on the basis of reactivity indices obtained by HOMO and LUMO energy Eigen values. Molecular electrostatic potential (MEP) plot has been presented to know about the different sites of electrophilic and nucleophilic attacks of the compound.

4. Result and discussion

Vibrational analysis

The optimized stable geometry and the scheme of atom numbering of the compound 2,3 d\Diphenyl-5-(thiophen-2-ylmethylidene)-2,5-dihydro-1,2,4-triazin-6(1H)-one is represented in Fig. 1. The optimized structural parameters bond length, bond angle and the dihedral angle for the more stable geometry of the title compound is determined at B3LYP with cc-pVDZ and cc-pVTZ basis sets are presented in Table 1. The impact of the substituent on the molecular parameters, mainly in the C-C bond distance of ring carbon atoms seems to be varied. The mean bond length of aromatic ring is 1.40 Å. The longer bond length (1.48 Å) of C11-C13 is due to the absence of delocalization of carbonyl lone pair of electrons towards the ring.

The observed and calculated FTIR and FT-Raman spectra of 2,3 d\Diphenyl-5-(thiophen-2-ylmethylidene)-2,5-dihydro-1,2,4-triazin-6(1H)-one are shown in Figs. 2 and 3 respectively. The observed FTIR and FT-Raman wavenumbers along with the theoretical IR and Raman wavenumbers along with their relative intensities and probable assignments are summarized in Table 2.

C–S, C–N and N–N vibrations

In the case of thiophene two C–S stretching vibrations are attributed, one is fell in higher wavenumber and another one is lower wavenumber. The C–S stretching wavenumbers are observed by Kwiatowski et al.[25, 26] at 840 and 754 cm^{-1} whereas Kupta et al.[27] have been predicted theoretically at 842 and 750 cm^{-1} by DFT method. In our present study, the ring connected C–S bond stretching vibration is calculated 821 cm^{-1} . The identification of C–N vibrations is very difficult because of the interference of many bands in the area where the vibration of this bond happens. For our title molecule, the C–N stretching appears in the region 1001-1520 cm^{-1} and the observed wavenumber (1002 cm^{-1}) is coinciding very well with calculated wavenumber (1001 cm^{-1}) in FT-IR. The electronegative nitrogen atom makes the carbon atom more positive and the polar -CN group has effect on the adjacent bond. C=N and N–N and each has a well-known characteristic vibrational frequency of its own parameters. N–N stretching vibration, which due to its symmetry has a very characteristic and they are difficult to observe in the infrared spectrum. Because of the change in dipole moment, the N–N bond length in the molecule also change in which has two abnormal C=N parts. These bands shift in wavenumber and intensity in a different way depending on the neighboring groups, H-bonding [28]. The substituents of title compound influence both the wavenumber and intensity. The medium band in FT-IR at 1234 cm^{-1} is accredited to the N–N stretching vibration of the molecule. The theoretical calculation by B3LYP method predicts the above said vibration at 1234 cm^{-1} exactly correlates with experimental findings.

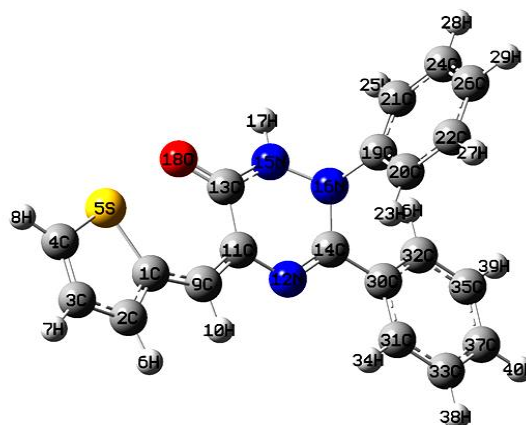


Fig. 1 Optimized geometrical structure and atom numbering of 2, 3-d\Diphenyl-5(thiophen-2-ylmethylidene)-2, 5-dihydro-1, 2, 4-triazin-6(1H)-one.

Table 1. Optimized structural parameters of 2,3-diphenyl-5-(thiophen-2-ylmethylidene)-2,5-dihydro-1,2,4-triazin-6(1H)-one utilizing B3LYP/cc-pVDZ and B3LYP/cc-pVTZ density functional calculation.

Parameter	Bond Length (Å)		Parameter	Bond Length (Å)		Parameter	Bond Angle (Å°)		Parameter	Bond Angle (Å°)		Parameter	Bond Angle (Å°)	
	B3LYP/ cc-pVDZ	B3LYP/ cc-pVTZ		B3LYP/ cc-pVDZ	B3LYP/ cc-pVTZ		B3LYP/ cc-pVDZ	B3LYP/ cc-pVTZ		B3LYP/ cc-pVDZ	B3LYP/ cc-pVTZ		B3LYP/ cc-pVDZ	B3LYP/ cc-pVTZ
C1-C2	1.39	1.39	C19-C20	1.40	1.40	C2-C1-S5	109.61	109.70	N12-C14-N16	123.62	122.92	C26-C24-H28	120.17	120.17
C1-S5	1.76	1.76	C19-C21	1.40	1.40	C2-C1-C9	121.31	121.34	N12-C14-C30	120.00	120.36	C22-C26-C24	119.78	119.62
C1-C9	1.44	1.44	C20-C22	1.40	1.40	S5-C1-C9	129.08	128.95	N16-C14-C30	116.37	116.72	C22-C26-H29	120.11	120.21
C2-C3	1.42	1.41	C20-H23	1.09	1.09	C1-C2-C3	114.32	114.19	C13-N15-N16	125.11	124.00	C24-C26-H29	120.10	120.17
C2-H6	1.09	1.08	C21-C24	1.40	1.39	C1-C2-H6	121.69	121.80	C13-N15-H17	118.27	117.53	C14-C30-C31	119.40	119.54
C3-C4	1.38	1.38	C21-H25	1.09	1.09	C3-C2-H6	123.99	124.01	N16-N15-H17	116.18	116.31	C14-C30-C32	121.64	121.45
C3-H7	1.09	1.08	C22-C26	1.40	1.40	C2-C3-C4	111.89	111.84	C14-N16-N15	112.11	113.27	C31-C30-C32	118.94	119.00
C4-S5	1.73	1.73	C22-H27	1.09	1.09	C2-C3-H7	124.20	124.24	C14-N16-C19	117.76	118.87	C30-C31-C33	120.46	120.42
C4-H8	1.09	1.08	C24-C26	1.40	1.40	C4-C3-H7	123.91	123.92	N15-N16-C19	113.27	113.82	C30-C31-H34	118.48	118.74
C9-H10	1.10	1.09	C24-H28	1.09	1.09	C3-C4-S5	112.79	112.81	N16-C19-C20	121.83	121.70	C33-C31-H34	121.06	120.84
C9-C11	1.37	1.37	C26-H29	1.09	1.09	C3-C4-H8	127.64	127.61	N16-C19-C21	118.17	118.44	C30-C32-C35	120.42	120.42
C11-N12	1.40	1.40	C30-C31	1.41	1.41	S5-C4-H8	119.57	119.57	C20-C19-C21	120.00	119.86	C30-C32-H36	119.53	119.61
C11-C13	1.48	1.48	C30-C32	1.41	1.40	C1-S5-C4	91.39	91.45	C19-C20-C22	119.75	119.82	C35-C32-H36	120.05	119.97
N12-C14	1.29	1.29	C31-C33	1.39	1.39	C1-C9-H10	112.17	112.22	C19-C20-H23	119.84	120.02	C31-C33-C37	120.25	120.26
C13-N15	1.37	1.37	C31-H34	1.09	1.08	C1-C9-C11	135.73	135.28	C22-C20-H23	120.40	120.16	C31-C33-H38	119.71	119.69
C13-O18	1.23	1.23	C32-C35	1.40	1.40	H10-C9-C11	112.07	112.44	C19-C21-C24	120.00	120.05	C37-C33-H38	120.04	120.05
C14-N16	1.42	1.42	C32-H36	1.09	1.08	C9-C11-N12	116.46	116.87	C19-C21-H25	119.40	119.75	C32-C35-C37	120.26	120.23
C14-C30	1.48	1.48	C33-C37	1.40	1.40	C9-C11-C13	124.88	125.18	C24-C21-H25	120.60	120.20	C32-C35-H39	119.65	119.63
N15-N16	1.41	1.41	C33-H38	1.09	1.09	N12-C11-C13	118.55	117.69	C20-C22-C26	120.34	120.42	C37-C35-H39	120.09	120.14
N15-H17	1.01	1.01	C35-C37	1.40	1.40	C11-N12-C14	121.11	120.80	C20-C22-H27	119.54	119.41	C33-C37-C35	119.67	119.68
N16-C19	1.45	1.45	C35-H39	1.09	1.09	C11-C13-N15	113.32	114.07	C26-C22-H27	120.12	120.16	C33-C37-H40	120.17	120.16

Table 2. Experimental and Calculated B3LYP/ cc-pVDZ and B3LYP/cc-pVTZ levels of vibrational frequencies (cm^{-1}), of 2,3-diphenyl-5-(thiophen-2-ylmethylidene)-2,5-dihydro-1,2,4-triazin-6(1H)-one.

S.No.	Observed frequency (cm^{-1})		Calculated frequency (cm^{-1})				Vibrational assignment/ (%)
	FT-IR	FT-Raman	Unscaled		Scaled		
			B3LYP/ cc-pVDZ	B3LYP/ cc-pVTZ	B3LYP/ cc-pVDZ	B3LYP/ cc-pVTZ	
1.	3250		3496	3603	3255	3251	vNH(96)
2.		3099	3243	3240	3094	3098	vCH(98)
3.	3078		3242	3218	3075	3076	vCH(98)
4.		3063	3222	3216	3060	3065	vCH(98)
5.	3031		3220	3215	3033	3034	vCH(97)
6.			3211	3207	3021	3024	vCH(98)
7.	3009		3205	3201	3010	3010	vCH(96)
8.	3002		3202	3200	3004	3003	vCH(96)
9.			3199	3197	2991	2992	vCH(98)
10.	2984		3187	3191	2985	2983	vCH(98)
11.			3186	3184	2962	2960	vCH(96)
12.	2937		3178	3182	2936	2937	vCH(95)
13.			3174	3175	2879	2882	vCH(95)
14.	2859		3165	3174	2860	2860	vCH(98)
15.	2835		3156	3154	2835	2836	vCH(98)
16.		1689	1776	1753	1688	1690	vCO(88)
17.	1671		1678	1668	1670	1671	vCC(80), δ CH(19)
18.		1627	1656	1654	1627	1626	vCC(80), δ CH(18)
19.	1609		1651	1647	1610	1609	vCC(81), δ CH(17)
20.		1598	1650	1637	1594	1598	vCC(69), δ CN(12), δ CH(10), δ NH(10)
21.	1578	1580	1626	1631	1576	1579	vCC(69), δ CH(12)
22.		1522	1561	1617	1520	1523	vCN(67), vCC(16), δ NH(10)
23.			1546	1544	1515	1516	vCC(68), δ CH(18), δ NH(11)
24.			1542	1520	1509	1510	δ NH(88)
25.		1501	1524	1518	1500	1501	vCC(86), δ CH(18)
26.	1484		1519	1479	1483	1485	δ CH(76), vCC(18)
27.		1441	1478	1475	1440	1441	δ CH(71), vCC(16)
28.	1421		1471	1470	1420	1422	δ CH(69), δ NH(11), vCC(10)
29.		1413	1465	1435	1414	1412	vCC(66), δ CH(17)
30.			1415	1409	1388	1384	vNN(66), vCN(19), δ NH(10)
31.	1375		1410	1365	1376	1376	δ CH(79)
32.	1348	1346	1365	1362	1345	1347	vCC(68), δ CH(18)
33.	1328		1363	1356	1326	1328	vCC(67), δ CH(19)
34.		1321	1350	1351	1320	1321	δ CH(69)

35.	1296		1331	1326	1295	1297	$\delta\text{CH}(73)$
36.	1284		1327	1322	1280	1282	$\delta\text{CH}(73)$
37.	1234		1310	1300	1231	1234	$v\text{CC}(66), v\text{CN}(12), v\text{NN}(10)$
38.		1225	1273	1263	1220	1225	$v\text{CC}(65), \delta\text{CH}(18)$
39.	1173		1253	1248	1170	1173	$\delta\text{CH}(66)$
40.			1247	1228	1152	1155	$\delta\text{CH}(66), v\text{CC}(12)$
41.			1195	1210	1148	1149	$\delta\text{CH}(65), v\text{CC}(10)$
42.		1144	1189	1187	1142	1144	$v\text{CC}(65), v\text{CC}(11)$
43.	1115		1189	1185	1113	1117	$v\text{CC}(67), v\text{CC}(11)$
44.		1109	1171	1171	1110	1110	$\delta\text{CH}(67), v\text{CC}(12)$
45.			1169	1170	1091	1093	$\delta\text{CH}(66), v\text{CC}(10)$
46.		1082	1143	1148	1083	1082	$v\text{CN}(65), v\text{CC}(11)$
47.	1062		1108	1100	1063	1062	$\delta\text{CH}(60), v\text{CC}(16)$
48.		1056	1101	1098	1055	1056	$\delta\text{CH}(63), v\text{CC}(16)$
49.	1039	1039	1088	1086	1039	1036	$\delta\text{CH}(66), v\text{CC}(12)$
50.			1073	1073	1020	1022	$\delta\text{CH}(65)$
51.	1002	1001	1062	1057	1001	1002	$v\text{CN}(60), \delta\text{CO}(17), v\text{CC}(11)$
52.			1050	1049	994	995	$\delta\text{ring}(70)$
53.			1048	1037	989	989	$\delta\text{ring}(71)$
54.			1022	1017	985	983	$\gamma\text{CH}(88)$
55.			1014	1015	979	976	$\delta\text{ring}(71)$
56.			1009	1014	963	960	$\delta\text{ring}(70), \delta\text{CH}(12)$
57.	957		1008	1012	957	955	$\gamma\text{CH}(69), \gamma\text{CC}(16)$
58.			998	998	942	940	$\gamma\text{CH}(66), \gamma\text{CC}(15)$
59.			973	986	931	932	$\gamma\text{CH}(66), \gamma\text{CC}(15)$
60.			966	970	919	920	$\gamma\text{CH}(65), \gamma\text{CC}(17)$
61.		912	949	954	910	911	$\gamma\text{CH}(65), \gamma\text{ring}(18)$
62.	906		926	940	905	907	$v\text{CC}(66), \delta\text{ring}(18)$
63.	890		923	937	895	890	$\gamma\text{CH}(66)$
64.			903	918	881	880	$\gamma\text{CH}(65)$
65.	828		873	867	829	830	$\gamma\text{CH}(65)$
66.			863	864	821	823	$v\text{CS}(67), \delta\text{CH}(12)$
67.		818	856	853	815	817	$\gamma\text{NH}(60)$
68.			839	836	808	810	$\gamma\text{CH}(67)$
69.			834	831	801	804	$\gamma\text{CH}(68)$
70.			819	806	797	799	$\delta\text{ring}(69), \delta\text{NH}(12)$
71.			802	791	788	788	$\gamma\text{CH}(61), \gamma\text{CC}(11)$
72.	781		794	776	780	781	$\gamma\text{CO}(62), \gamma\text{CC}(13), \gamma\text{CN}(10)$
73.			778	754	761	760	$\gamma\text{CH}(66)$
74.		741	770	748	745	742	$\gamma\text{CH}(54), \delta\text{ring}(18)$
75.	734		744	731	735	734	$\delta\text{ring}(55)$
76.			724	719	720	718	$\gamma\text{CH}(55)$
77.			713	713	706	705	$\gamma\text{CH}(61)$
78.			712	712	693	695	$\gamma\text{CH}(60)$

79.		687	707	706	685	683	γ CH(61)
80.	656		701	683	655	653	γ CN(58), γ ring(12)
81.			682	643	637	636	δ ring(51), δ NH(15)
82.		625	649	630	624	625	δ NH(61)
83.			630	627	617	618	δ ring(55)
84.			627	614	608	609	δ ring(58)
85.		599	615	596	600	598	δ ring(55)
86.	593		595	581	590	592	γ NN(58)
87.	562		593	566	560	562	γ ring(58)
88.			562	522	533	530	γ ring(55)
89.			524	515	504	504	γ CC(61), γ ring(11)
90.			507	510	489	490	γ CH(60), γ ring(12)
91.			494	466	461	462	γ ring(61), γ NH(50)
92.			447	449	413	410	δ CC(61)
93.			422	429	407	405	γ CC(60), γ ring(12)
94.			416	420	400	402	γ ring(61)
95.			414	418	386	385	γ ring(60)
96.			361	363	341	340	γ ring(58), γ CC(12)
97.			353	353	322	321	γ CC(51)
98.			329	340	301	300	γ CN(53)
99.		283	286	295	283	282	δ CO(52)
100.			258	275	240	242	δ CC(50)
101.			242	250	223	220	γ NH(55), γ CO(13)
102.			220	214	202	201	γ CC(76), γ ring(10)
103.			207	209	189	189	γ CC(61)
104.			185	175	167	165	γ NH(62)
105.			152	148	139	140	γ CC(62)
106.		127	140	136	125	130	γ CN(60)
107.		89	97	93	88	88	γ CO(60)
108.			79	73	77	75	γ CC(58)
109.			71	58	70	71	γ CN(58)
110.			43	46	42	40	γ CC(51)
111.			38	41	38	36	γ ring(53)
112.			35	24	33	31	γ ring(52)
113.			25	17	24	24	γ ring(52)
114.			19	15	20	20	γ ring(48)

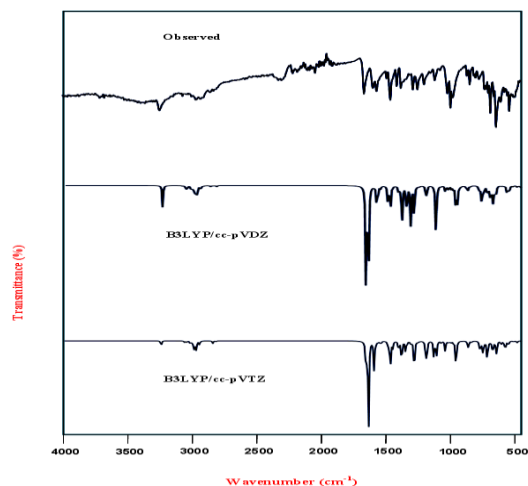


Fig. 2 Observed and simulated infrared spectra of 2, 3-diphenyl-5-(thiophen-2-ylmethylidene)-2, 5-dihydro-1, 2, 4-triazin-6(1H)-one.

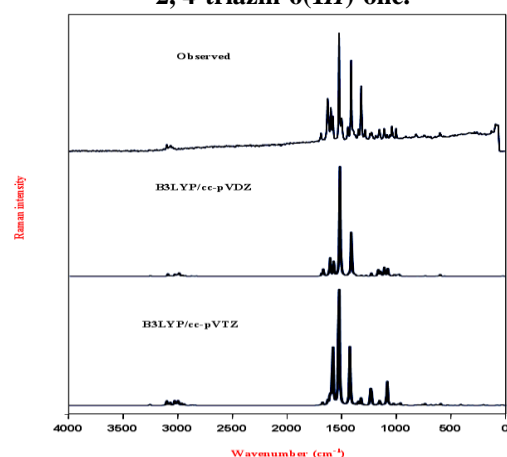


Fig. 3 Observed and simulated Raman spectra of 2, 3-diphenyl-5-(thiophen-2-ylmethylidene)-2, 5-dihydro-1, 2, 4-triazin-6(1H)-one.

C = O vibrations

The carbonyl stretching frequency is very sensitive to the factors that disturb the nature of the carbonyl group and its precise frequency is characteristic of the type of the carbonyl compound being studied. This region is considered as a very important region by organic chemists. The carbonyl stretching vibrations in ketones are expected in the region 1715-1680 cm^{-1} [29]. The carbon oxygen double bond is formed by $\pi - \pi$ between carbon and oxygen, and the lone pair of electron on oxygen also determines the nature of the carbonyl group. For our present study, the band caused by C=O stretching vibration is observed in the region 1689 cm^{-1} in FT-Raman is very much correlated with calculated wavenumber 1688 cm^{-1} . If the spectrum contains a strong absorption band between 1900-1600 cm^{-1} , the carbonyl group (C=O) will be presented in a compound. The position of the peak or the band not only tells the presence of a particular group but also reveals a good deal about the environments affecting the group.[30]

C-C and C-H vibrations

The aromatic ring vibrational modes of the title molecule have been verified based on the vibrational spectra of previously published vibrations of the benzene molecule are helpful in the identification of the phenyl ring modes [31]. The ring stretching vibrations are very prominent, as the double bond is in conjugation with the ring, in the vibrational spectra of benzene and its derivatives[32]. The ring carbon-carbon stretching vibrations occur in the region 1650-1450 cm^{-1} . In the title compound, the wavenumbers observed in the FT-IR spectrum at 1609, 1578, 1348, 1328

cm^{-1} have been assigned to C-C stretching vibrations. The theoretically computed values at 1610, 1576, 1515, 1414, 1345, 1326 cm^{-1} show the excellent agreement with the experimental data. The characteristic region for the identification of C-H stretching vibration, the heteroaromatic structure illustrated in the region 3100-3000 cm^{-1} . The calculated wavenumbers of the C-H symmetric stretching vibrations using B3LYP/cc-pVDZ in title molecule at 3094, 3075, 3060, 3033, 3021, 3010 and 3004 cm^{-1} are in good agreement with the experimental data. The C-H in-plane bending and C-H out-of-plane bending vibrations are normally found in the range 1300-1000 and 1000-750 cm^{-1} , respectively in aromatic compounds and are very useful for characterization purposes[33, 34]. The C-H in-plane bending vibrations are observed at 1484, 1421, 1375, 1296, 1156 cm^{-1} in FT-IR and the calculated wavenumbers are 1483, 1420, 1376, 1295, 1155 cm^{-1} that are well correlated with the experimental wavenumber. The C-H out-of-plane bending vibrations are calculated at 957, 910, 829, 685 cm^{-1} . The experimental values are assigned at 957, 912, 828, 687 cm^{-1} which show excellent agreement with calculated ones.

N-H Vibrations

In N-H stretching mode, the strong band of N-H stretching extends from 3400 to 3100 cm^{-1} , with the centre of the band at 3370 cm^{-1} [35-37]. The calculated wavenumber of the above mode is at 3255 cm^{-1} for the B3LYP/cc-pVDZ method. The strong band in the FT-IR spectrum at 3250 cm^{-1} also supports the formation of a strong N-H...N hydrogen bond. The lowering of the N-H stretching wavenumber can be attributed to the red shifting due to intermolecular N-H...N interaction. The red shifting is further enhanced by the reduction in the N-H bond order values, occurring due to donor-acceptor interaction. The first overtone of the N-H bending mode falling on the N-H stretching band positions produces two bands of comparable intensities, equally displaced on either side of this wavenumber resulting from Fermi resonance with one or more N-H stretching.

Frontier Molecular Orbitals

Highly occupied molecular orbital (HOMO) and Lowest unoccupied molecular orbital (LUMO) are the main orbital that take part in chemical stability. Molecular orbital's can provide insight into the nature of reactivity and some of the structural and physical properties. The HOMO represents the ability to donate an electron, while LUMO as an electron acceptor represents the ability to obtain an electron. The one electron excitation from HOMO and LUMO mainly described the electronic transition absorption correspond to the transition from ground to first excited state [38]. The energy gap between HOMO and LUMO has been used to prove the bioactivity from intramolecular charge transfer [39]. The energy gap measures the kinetic energy stability of the molecules. Considering the chemical hardness, large HOMO-LUMO gap means a hard molecule and small HOMO-LUMO gap means a soft molecule and also can relate the stability of the molecule to hardness, which means that increase of the HOMO-LUMO energy gap decreases reactivity of the compound that leads to increase in the stability of the molecule [40]. The frontier molecules orbital, HOMO and LUMO and frontier molecular energy gap helping the reactivity and kinetic stability of molecules are essential parameters in the electronic studies[41, 42]. From the Fig. 4, the energy values of HOMO (E_{HOMO}) and LUMO (E_{LUMO}) are -5.28736 and -1.98749 eV respectively. In the studied compound the HOMO-LUMO energy gap (ΔE) is 3.29987 eV that reflects the chemical reactivity of the

molecule. Using HOMO and LUMO orbital energies, the ionization energy and electron affinity can be expressed as: $I = -E_{\text{HOMO}} = 5.28736$ eV. $A = -E_{\text{LUMO}} = 1.98749$ eV. The hardness (η) and chemical potential (μ) are given the following formula $\eta = (I-A)/2$ and $\mu = -(I+A)/2$, where I and A are the first ionization potential and electron affinity of the chemical species. For the title compound, $E_{\text{HOMO}} = -5.28736$ eV, $E_{\text{LUMO}} = -1.98749$ eV, Energy gap = HOMO-LUMO = 3.29987 eV, Ionization potential (I) = 5.28736 eV, Electron affinity (A) = 1.98749 eV, Chemical hardness (η) = 1.64993 eV, Electronegativity (χ) = -3.637425 eV, Softness (s) = 0.606086 eV⁻¹, Chemical potential (μ) = 3.637425 eV, Electrophilicity index (ω) = 4.00952.

Fukui Functions

Fukui function is an indigenous reactivity identifier that predicts the ideal regions where a molecular fragment will change its density when the number of electrons is changed and it specified the tendency of the electronic density to deform at a given position upon accepting or donating electrons [43-45].

Also, it is probable to define the atomic Fukui functions on the j^{th} atom site

$$\begin{aligned} f_j^+ &= q_j(N+1) - q_j(N) \\ f_j^- &= q_j(N) - q_j(N-1) \\ f_j^0 &= \frac{1}{2}[q_j(N+1) - q_j(N-1)] \end{aligned}$$

For an electrophilic f_j^- (r), nucleophilic or free radical attack f_j^+ (r), on the reference molecule, respectively. In these equation, q_j is the atomic charge (evaluated from Mulliken population analysis, electrostatic derived charge, etc.) at the j^{th} atomic site is the neutral (N), anionic ($N+1$) or cationic ($N-1$) chemical species. Chattaraj et al. [46] proposed the idea of generalized philicity and it contains almost all information about the known different global and local reactivity and selectivity descriptor, in addition to the information regarding electrophilic/nucleophilic power of a given atomic site in a molecule. Morell et al. [47] have proposed a dual descriptor ($\Delta f(r)$), which is defined as the difference between the nucleophilic and electrophilic Fukui function and in given by,

$$\Delta f(r) = [f^+(r) - f^-(r)]$$

If $\Delta f(r) > 0$, then the site is favoured for a nucleophilic attack,

$\Delta f(r) < 0$, then the site may be favoured for an electrophilic attack.

Under this situation, the reactivity descriptor $\Delta f(r)$ provide useful information on both stabilising and destabilising interactions between a nucleophile and an electrophile and helps in identifying the electrophilic/nucleophilic behaviour of a specific site within a molecule. It provides positive value for site prone for

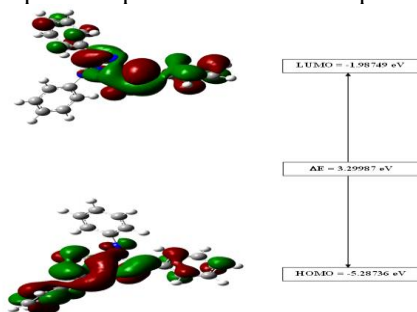


Fig. 4. HOMO- LUMO plot of 2, 3-diphenyl-5-(thiophen-2-ylmethylidene)-2, 5- dihydro- 1, 2, 4-triazin-6(1H)-one.

nucleophilic attack and a negative value prone for electrophilic attack and these values reported in Table. 3 according to the condition for dual descriptor, nucleophilic site for in our title molecule is C2, C3, H8, C9, C11, N13 (positive value i.e. $\Delta f(r) > 0$). Similarly, the electrophilic site is C1, C4, S5, H6, H7, H10, C12, C14, N15, O16, N17, H18, C19, H20, C21, C22, H23, C24, H25, C26, H27, H28, H29, C30, C31, C32, C33, H34, C35, H36, C37, H38, H39, H40 (Negative i.e. $\Delta f(r) < 0$). The behaviour of molecules as electrophiles/nucleophiles during reaction depends on the local behaviour of molecules.

NBO analysis

Natural bond orbital analysis gives a measurable method for studying intra and intermolecular bonding and interaction among bonds, and also gives a appropriate basis for examining charge transfer or conjugative interactions in molecular systems. NBO method gives useful information about interactions in both filled and virtual orbital spaces which could enhance the analysis of intra and intermolecular interactions [48]. Estimating their energy importance by second order perturbation theory and considering all possible interactions between filled donor and empty acceptor NBOs. The second order Fock matrix was carried out to evaluate the donor-acceptor interactions in the NBO analysis. The change in electron density (ED) in the (σ^* , π^*) antibonding orbitals and E(2) energies have been calculated by natural bond orbital (NBO) analysis using DFT method to give clear evidence of stabilization originating from various molecular interactions. Delocalization of electron density between occupied Lewis type (bond or lone pair) NBO orbitals and formally unoccupied (antibonding or Rydberg) non-Lewis NBO orbitals correspond to a stabilizing donor acceptor interaction. Accumulation of natural charges and electron population of atoms in core, valance, Rydberg orbitals of 2,3-diphenyl-5-(thiophen-2-ylmethylidene)-2,5-dihydro-1,2,4-triazin-6(1H)-one is calculated and shown in Table. 4

The stabilization energy E(2) is estimated as

$$E(2) = \Delta E_{ij} = q_i \frac{F(i,j)^2}{\epsilon_j - \epsilon_i}$$

where i is the donor and j is the acceptor associated with E(2).

Some electron donor orbital, acceptor orbital and the interacting stabilization energy resulting from the second order micro-disturbance theory are reported where q_i is the donor orbital occupancy, ϵ_i and ϵ_j are diagonal elements and $F(i,j)$ is the off diagonal NBO second-order Fock matrix element reported [49, 50]. The larger E(2) value, the more intensive is the interaction among electron donors and acceptors, i.e. the high donating tendency from electron donors to electron acceptors and the greater the extent on formation of the whole system. NBO analysis was performed on the molecule at the DFT/B3LYP/cc-pVTZ level in order to elucidate the intra molecular rehybridization and delocalization of electron density within the molecule [51]. In this study, the intramolecular hyperconjugative (interaction of the electrons in a sigma bond) interaction of $\sigma(C_1-C_2)$ distributed to $\sigma^*(C_3-H_8)$ resulting the stabilization energy of 3.16 kcal/mole are shown in Table. 5. This improved further conjugation with the $\pi^*(C_1 - C_2)$ antibonding orbital with a stabilization energy of 65.21 kcal/mole. In the title compound, the $\pi(C_{14}) \rightarrow \pi^*(C_{30} - C_{31})$, $\pi^*(C_{11} - N_{13})$ and $\pi(C_3) \rightarrow \pi^*(C_4 - C_9)$ show stabilization energies of 40.11 kcal/mole, 57.22 kcal/mole and 74.3 kcal/mole respectively.

Table 3. Values of Fukui function considering Mulliken charges of 2,3-diphenyl-5-(thiophen-2-ylmethylidene)-2,5-dihydro-1,2,4-triazin-6(1H)-one.

Mulliken Atomic Charges (a.u)			Fukui's Function (a.u)					Atomic Softness			Electrophilicity Indices		
Atom	Neutral (N)	Cation (N-1)	Anion (N+1)	f_k^+	f_k^-	f_k°	$\Delta f(r)$	s_k^+	s_k^-	s_k°	ω_k^+	ω_k^-	ω_k°
C1	-0.173753	-0.459	-0.624	-0.4502	0.28525	-0.0825	-0.7355	-0.173	0.110	-0.032	-1.472	0.933	-0.2698
C2	-0.127572	0.156	0.026	0.15357	-0.2836	-0.065	0.43714	0.059	-0.109	-0.025	0.502	-0.927	-0.2126
C3	-0.149615	-0.015	-0.136	0.01362	-0.1346	-0.0605	0.14823	0.005	-0.052	-0.023	0.045	-0.440	-0.1978
C4	0.047176	-0.103	-0.173	-0.2202	0.15018	-0.035	-0.3704	-0.085	0.058	-0.013	-0.720	0.491	-0.1145
S5	0.169374	0.214	0.028	-0.1414	-0.0446	-0.093	-0.0967	-0.054	-0.017	-0.036	-0.462	-0.146	-0.3041
H6	0.134155	0.212	0.027	-0.1072	-0.0778	-0.0925	-0.0293	-0.041	-0.030	-0.036	-0.350	-0.255	-0.3025
H7	0.124401	-0.499	-0.666	-0.7904	0.6234	-0.0835	-1.4138	-0.304	0.240	-0.032	-2.585	2.039	-0.273
H8	0.121516	0.352	0.246	0.12448	-0.2305	-0.053	0.35497	0.048	-0.089	-0.020	0.407	-0.754	-0.1733
C9	-0.117912	0.362	0.235	0.35291	-0.4799	-0.0635	0.83282	0.136	-0.185	-0.024	1.154	-1.569	-0.2076
H10	0.13615	0.159	-0.196	-0.3322	-0.0229	-0.1775	-0.3093	-0.128	-0.009	-0.068	-1.086	-0.075	-0.5804
C11	-0.011716	0.831	0.737	0.74872	-0.8427	-0.047	1.59143	0.288	-0.325	-0.018	2.448	-2.756	-0.1537
C12	0.127944	-0.019	-0.037	-0.1649	0.14694	-0.009	-0.3119	-0.064	0.057	-0.003	-0.539	0.481	-0.0294
N13	-0.245287	0.555	0.492	0.73729	-0.8003	-0.0315	1.53757	0.284	-0.308	-0.012	2.411	-2.617	-0.103
C14	0.093139	-0.236	-0.301	-0.3941	0.32914	-0.0325	-0.7233	-0.152	0.127	-0.013	-1.289	1.076	-0.1063
N15	-0.005492	-0.257	-0.315	-0.3095	0.25151	-0.029	-0.561	-0.119	0.097	-0.011	-1.012	0.822	-0.0948
O16	-0.248589	-0.254	-0.314	-0.0654	0.00541	-0.03	-0.0708	-0.025	0.002	-0.012	-0.214	0.018	-0.0981
N17	-0.242846	-0.267	-0.323	-0.0802	0.02415	-0.028	-0.1043	-0.031	0.009	-0.011	-0.262	0.079	-0.0916
H18	0.153837	-0.276	-0.3295	-0.4833	0.42984	-0.0268	-0.9132	-0.186	0.166	-0.010	-1.581	1.406	-0.0875
C19	0.179381	-0.285	-0.336	-0.5154	0.46438	-0.0255	-0.9798	-0.198	0.179	-0.010	-1.685	1.519	-0.0834
H20	0.204925	-0.294	-0.3425	-0.5474	0.49893	-0.0243	-1.0464	-0.211	0.192	-0.009	-1.790	1.631	-0.0793
C21	-0.13545	-0.303	-0.349	-0.2136	0.16755	-0.023	-0.3811	-0.082	0.065	-0.009	-0.698	0.548	-0.0752
C22	-0.098462	-0.312	-0.3555	-0.257	0.21354	-0.0218	-0.4706	-0.099	0.082	-0.008	-0.841	0.698	-0.0711
H23	0.099709	-0.321	-0.362	-0.4617	0.42071	-0.0205	-0.8824	-0.178	0.162	-0.008	-1.510	1.376	-0.067
C24	-0.097705	-0.33	-0.3685	-0.2708	0.2323	-0.0193	-0.5031	-0.104	0.089	-0.007	-0.885	0.760	-0.0629
H25	0.114526	-0.339	-0.375	-0.4895	0.45353	-0.018	-0.9431	-0.189	0.175	-0.007	-1.601	1.483	-0.0589
C26	-0.108431	-0.348	-0.3815	-0.2731	0.23957	-0.0168	-0.5126	-0.105	0.092	-0.006	-0.893	0.783	-0.0548
H27	0.103508	-0.357	-0.388	-0.4915	0.46051	-0.0155	-0.952	-0.189	0.177	-0.006	-1.607	1.506	-0.0507
H28	0.104788	-0.366	-0.3945	-0.4993	0.47079	-0.0143	-0.9701	-0.192	0.181	-0.005	-1.633	1.539	-0.0466
H29	0.103752	-0.375	-0.401	-0.5048	0.47875	-0.013	-0.9835	-0.194	0.184	-0.005	-1.651	1.566	-0.0425
C30	0.070184	-0.384	-0.4075	-0.4777	0.45418	-0.0118	-0.9319	-0.184	0.175	-0.005	-1.562	1.485	-0.0384
C31	-0.134765	-0.393	-0.414	-0.2792	0.25824	-0.0105	-0.5375	-0.108	0.099	-0.004	-0.913	0.844	-0.0343
C32	-0.093252	-0.402	-0.4205	-0.3272	0.30875	-0.0092	-0.636	-0.126	0.119	-0.004	-1.070	1.010	-0.0302
C33	-0.109552	-0.411	-0.427	-0.3174	0.30145	-0.008	-0.6189	-0.122	0.116	-0.003	-1.038	0.986	-0.0262
H34	0.094887	-0.42	-0.4335	-0.5284	0.51489	-0.0068	-1.0433	-0.203	0.198	-0.003	-1.728	1.684	-0.0221
C35	-0.100586	-0.429	-0.44	-0.3394	0.32841	-0.0055	-0.6678	-0.131	0.126	-0.002	-1.110	1.074	-0.018
H36	0.114661	-0.438	-0.4465	-0.5612	0.55266	-0.0043	-1.1138	-0.216	0.213	-0.002	-1.835	1.807	-0.0139
C37	-0.109888	-0.447	-0.453	-0.3431	0.33711	-0.003	-0.6802	-0.132	0.130	-0.001	-1.122	1.102	-0.0098
H38	0.105512	-0.456	-0.4595	-0.565	0.56151	-0.0018	-1.1265	-0.218	0.216	-0.001	-1.848	1.836	-0.0057
H39	0.107663	-0.465	-0.466	-0.5737	0.57266	-0.0005	-1.1463	-0.221	0.221	0.000	-1.876	1.873	-0.0016
H40	0.106442	-0.474	-0.4725	-0.5789	0.58044	0.00075	-1.1594	-0.223	0.224	0.000	-1.893	1.898	0.00245

Table 4. Accumulation of natural charges and electron population of atoms in core, valence, Rydberg orbitals of 2,3-diphenyl-5-(thiophen-2-ylmethylidene)-2,5-dihydro-1,2,4-triazin-6(1H)-one.

Atoms ^a	Charge (e)	Natural population (e)			Total (e)	Atoms ^b	Charge (e)	Natural population (e)			Total (e)
		Core	Valence	Rydberg				Core	Valence	Rydberg	
S5	0.49999	9.99871	5.45335	0.04795	15.50001	C1	-0.39006	1.99926	4.36810	0.02270	6.39006
H6	0.23045	0.00000	0.76759	0.00195	0.76955	C2	-0.23613	1.99926	4.21823	0.01864	6.23613
H7	0.21840	0.00000	0.77965	0.00196	0.78160	C3	-0.20934	1.99912	4.19191	0.01831	6.20934
H8	0.22017	0.00000	0.77786	0.00197	0.77983	C4	-0.25350	1.99914	4.22751	0.02685	6.25350
H10	0.20350	0.00000	0.79302	0.00348	0.79650	C9	-0.07243	1.99922	4.05306	0.02016	6.07243
C11	0.00280	1.99917	3.96569	0.03234	5.99720	N13	-0.46381	1.99948	5.43675	0.02758	7.46381
C12	0.56043	1.99911	3.40423	0.03623	5.43957	N15	-0.25465	1.99930	5.23108	0.02427	7.25465
C14	0.38931	1.99925	3.58717	0.02427	5.61069	O16	-0.53903	1.99973	6.50715	0.03215	8.53903
H18	0.38130	0.00000	0.61432	0.00438	0.61870	N17	-0.47408	1.99941	5.45012	0.02455	7.47408
C19	0.13518	1.99895	3.84424	0.02163	5.86482	C20	-0.19713	1.99910	4.17941	0.01861	6.19713
H23	0.21227	0.00000	0.78502	0.00271	0.78773	C21	-0.21177	1.99910	4.19552	0.01715	6.21177
H25	0.21149	0.00000	0.78624	0.00227	0.78851	C22	-0.19197	1.99924	4.17519	0.01754	6.19197
H27	0.20541	0.00000	0.79257	0.00203	0.79459	C24	-0.19397	1.99924	4.17712	0.01760	6.19397
H28	0.20493	0.00000	0.79304	0.00203	0.79507	C26	-0.20205	1.99924	4.18471	0.01809	6.20205
H29	0.20396	0.00000	0.79410	0.00194	0.79604	C30	-0.09173	1.99899	4.07100	0.02175	6.09173
H34	0.20562	0.00000	0.79166	0.00273	0.79438	C31	-0.19769	1.99914	4.18125	0.01730	6.19769
H36	0.23188	0.00000	0.76560	0.00251	0.76812	C32	-0.16595	1.99915	4.14906	0.01775	6.16595
H38	0.20487	0.00000	0.79312	0.00200	0.79513	C33	-0.19508	1.99924	4.17832	0.01752	6.19508
H39	0.20608	0.00000	0.79190	0.00202	0.79392	C35	-0.19584	1.99924	4.17861	0.01799	6.19584
H40	0.20386	0.00000	0.79414	0.00200	0.79614	C37	-0.19569	1.99924	4.17782	0.01863	6.19569

^aAtoms containing positive charges^bAtoms containing negative charges

Table 5. Significant second-order interaction energy (E (2), kcal/mol) between donor and acceptor orbitals of 2,3-diphenyl-5-(thiophen-2-ylmethylidene)-2,5-dihydro-1,2,4-triazin-6(1H)-one calculated at B3LYP/cc-pVTZ level of theory.

Donor (i)	Acceptor (j)	E(2) ^a kcal/mol	($\epsilon_i - \epsilon_j$) ^b a.u	F_{ij} ^c a.u	Donor (i)	Acceptor (j)	E(2) ^a kcal/mol	($\epsilon_i - \epsilon_j$) ^b a.u	F_{ij} ^c a.u	Donor (i)	Acceptor (j)	E(2) ^a kcal/mol	($\epsilon_i - \epsilon_j$) ^b a.u	F_{ij} ^c a.u
σ (C1-C2)	σ^* (C3-H8)	3.16	1.14	0.054	σ (C19-C20)	σ^* (C21-C24)	20.69	0.28	0.068	σ (C32-H36)	σ^* (C30-C31)	5.41	1.03	0.067
σ (C1-S5)	σ^* (C2-H7)	4.31	1.1	0.062	σ (C19-C20)	σ^* (C22-C26)	19.86	0.28	0.067	σ (C32-H36)	σ^* (C35-C37)	4.6	1.04	0.062
σ (C1-S5)	σ^* (C4-C9)	5.4	1.1	0.069	σ (C20-C22)	σ^* (N17-C19)	4.93	1.05	0.064	σ (C33-C37)	σ^* (C30-C31)	20.4	0.28	0.068
σ (C1-H6)	σ^* (C2-C3)	3.09	1.04	0.051	σ (C20-H23)	σ^* (C19-C21)	4.95	1.05	0.064	σ (C33-C37)	σ^* (C32-C35)	18.88	0.28	0.066
σ (C2-C3)	σ^* (C1-H6)	3.92	1.08	0.058	σ (C20-H23)	σ^* (C22-C26)	4.23	1.05	0.06	σ (C33-H38)	σ^* (C30-C31)	5.03	1.04	0.065
σ (C2-C3)	σ^* (C4-C9)	5.87	1.08	0.071	σ (C21-C24)	σ^* (N17-C19)	4.79	1.05	0.064	σ (C33-H38)	σ^* (C35-C37)	4.54	1.05	0.062
σ (C2-H7)	σ^* (C1-S5)	3.83	0.77	0.049	σ (C21-C24)	σ^* (C19-C20)	20.87	0.28	0.069	σ (C35-H39)	σ^* (C30-C32)	4.93	1.05	0.064
σ (C3-C4)	σ^* (C2-H7)	3.28	1.13	0.055	σ (C21-C24)	σ^* (C22-C26)	20.41	0.28	0.068	σ (C35-H39)	σ^* (C33-C37)	4.6	1.05	0.062
σ (C3-H8)	σ^* (C4-S5)	4.87	0.77	0.055	σ (C21-H25)	σ^* (C19-C20)	4.85	1.06	0.064	σ (C37-H40)	σ^* (C31-C33)	4.6	1.05	0.062
σ (C4-S5)	σ^* (C1-H6)	3.58	1.1	0.056	σ (C21-H25)	σ^* (C24-C26)	4.19	1.06	0.06	σ (C37-H40)	σ^* (C32-C35)	4.53	1.06	0.062
σ (C4-S5)	σ^* (C3-H8)	3.99	1.1	0.059	σ (C22-C26)	σ^* (C19-C20)	20.76	0.28	0.068	π (C3)	π^* (C1-C2)	65.21	0.12	0.096
σ (C4-C9)	σ^* (C11-C12)	3.7	0.77	0.051	σ (C22-C26)	σ^* (C21-C24)	20.6	0.28	0.068	π (C3)	π^* (C4-C9)	74.3	0.11	0.095
σ (C4-C9)	σ^* (C11-N13)	3.29	0.74	0.049	σ (C22-H27)	σ^* (C19-C20)	4.7	1.05	0.063	π (S5)	π^* (C1-C2)	27.19	0.25	0.075
σ (C9-H10)	σ^* (C4-S5)	5.35	0.77	0.057	σ (C22-H27)	σ^* (C24-C26)	4.59	1.05	0.062	π (S5)	π^* (C4-C9)	27.39	0.24	0.072
σ (C9-H10)	σ^* (C11-N13)	3.24	0.54	0.043	σ (C24-H28)	σ^* (C19-C21)	4.69	1.05	0.063	π (N13)	π^* (C11-C12)	6.4	0.89	0.068
σ (C9-C11)	σ^* (C3-C4)	3.31	1.19	0.056	σ (C24-H28)	σ^* (C22-C26)	4.57	1.05	0.062	π (N13)	π^* (C14-N15)	8.56	0.74	0.071
σ (C11-C12)	σ^* (C12-O16)	3.69	1.45	0.066	σ (C26-H29)	σ^* (C20-C22)	4.54	1.05	0.062	π (C14)	π^* (C11-N13)	57.22	0.13	0.089
σ (C11-C12)	σ^* (N15-N17)	5.34	0.98	0.065	σ (C26-H29)	σ^* (C21-C24)	4.57	1.05	0.062	π (C14)	π^* (C30-C31)	40.11	0.15	0.084
σ (C11-N13)	σ^* (C14-C30)	5.44	1.16	0.071	σ (C30-C31)	σ^* (C32-C35)	18.87	0.29	0.067	π (N15)	π^* (C12-O16)	43.98	0.32	0.107
σ (C11-N13)	σ^* (C9-H10)	3.13	0.71	0.044	σ (C30-C31)	σ^* (C33-C37)	19.73	0.28	0.067	π (N15)	π^* (N17-H18)	5.43	0.68	0.06
σ (C11-N13)	σ^* (C12-O16)	18.77	0.34	0.074	σ (C31-C33)	σ^* (C14-C30)	4.41	1.09	0.062	π (O16)	π^* (C11-C12)	25.84	0.76	0.128
σ (C12-N15)	σ^* (C14-C30)	4.01	1.16	0.061	σ (C31-H34)	σ^* (C30-C32)	4.74	1.06	0.063	π (O16)	π^* (C12-N15)	41.66	0.63	0.147
σ (C12-O16)	σ^* (C11-N13)	5.36	0.39	0.047	σ (C31-H34)	σ^* (C33-C37)	4.16	1.06	0.059	π (N17)	π^* (C12-N15)	6.83	0.65	0.059
σ (N13-C14)	σ^* (C9-C11)	5.54	1.23	0.074	σ (C32-C35)	σ^* (C14-C30)	4.04	1.09	0.059	π (N17)	π^* (C14-N15)	5.28	0.62	0.052
σ (N13-C14)	σ^* (N15-N17)	4.69	1.09	0.064	σ (C32-C35)	σ^* (C30-C31)	20.25	0.27	0.068	π (N17)	π^* (C19-C20)	5.43	0.81	0.061
σ (C14-N15)	σ^* (C12-O16)	3.53	1.56	0.066	σ (C32-C35)	σ^* (C33-C37)	21.23	0.28	0.068	π (N17)	π^* (C19-C20)	5.08	0.29	0.036
										π (N17)	π^* (C19-C21)	5.36	0.8	0.06

Molecular electrostatic potential (MEP)

Molecular electrostatic potential provides a visual method to understand the relative polarity of the molecule. MEP is in valuable tool in predicting and analysing the molecular interactions such as Drug – receptor and enzyme – substrate interactions. MEP is very helpful for the qualitative elucidation of electrophilic and nucleophilic reactions for the study of biological discovery process and hydrogen bonding interactions [52]. An electron density iso-surface mapped with electrostatic potential surface depicts the size, shape, charge density and site of chemical reactivity of the molecule.

From the MEP picture, oxygen has higher electronegativity value than nitrogen and sulphur. Oxygen atom would consequently possess higher electric density around it, than nitrogen and sulphur atoms. Thus, the spherical region that corresponds to an oxygen atom would have a red position on it. However, the light-yellow region spread on the MEP surface due to potential halfway between the two extreme regions and this confirms the existence of an intermolecular interaction.

To predict the reactive sites of electrophilic and nucleophilic attack for the investigated molecule, the MEP at the B3LYP/cc-pVDZ optimized geometry was calculated and shown in Fig. 5a. The MEP is related to the electronic density and is very useful descriptor for determining sites for electrophilic attack and nucleophilic reactions as well as hydrogen-bonding interactions[53-56]. The negative (red and yellow) regions of MEP were related to electrophilic reactivity and the positive (blue) regions to nucleophilic reactivity as shown in Fig. 5b. These are two possible sites of electrophilic attack. The negative regions are mainly localized on the carbonyl oxygen atoms and also a negative electrostatic potential region is observed around the N atom. The Fig. 5b confirms the existence of an intermolecular N-H---N interaction between the protonated (addition of a proton (H+) to an atom or molecule) and unprotonated N, O and S atoms. The molecular electrostatic potential map shows that the positive potential sites are around the hydrogen atoms and negative potential sites are on electronegative atoms. These sites give information about the region from where the compound can have noncovalent interactions.

Non-Linear optical activity

Highly NLO active molecular materials are attracting wide interest because of their potential applications in opto electronic devices of telecommunications, information storage, optical switching signal processing[57, 58] and THz wave generation[59]. THz region which lies between microwaves and infrared region of the electromagnetic spectrum, offers diverse applications such as wireless communications, inspection of drugs, spectroscopy and imaging[60]. Due to measures in the field of technology, there is an increasing interest in designing new organic materials with desired nonlinear optical properties.

The dipole moment (μ), the static polarizability (α_0) and first static hyperpolarizability (β_{tot}) are related directly to the non-linear optical (NLO) activity of molecular structures. NLO activities of molecules have also reverse relationship with their biological activities.

The calculated values of the polarizabilities and the hyper polarizabilities from Gaussian 09 output were converted from atomic units into electrostatic units [61]. The total dipole moment (μ) = $(\mu_x^2 + \mu_y^2 + \mu_z^2)^{1/2}$

$$\langle \alpha \rangle = 1/3 (\alpha_{xx} + \alpha_{yy} + \alpha_{zz})$$

and first static hyper polarizability (β_{tot}) from Gaussian output,[62]

$$\beta_{tot} = [(\beta_{xxx} + \beta_{xyy} + \beta_{xzz})^2 + (\beta_{yyy} + \beta_{yzz} + \beta_{yxx})^2 + (\beta_{zzz} + \beta_{zxx} + \beta_{zyy})^2]^{1/2}$$

The calculated (β_{tot}) & $\langle \alpha \rangle$ and ground state dipole moment were computed to be 7.739×10^{-30} esu and -137.64183 esu.

According to the Table. 6, B3LYP/cc-pVTZ results are listed as the electronic dipole moment μ_i ($i = x, y, z$) polarizability α_0 and the first hyperpolarizability β_0 for the title compound. The calculated dipole moment is equal to 1.3054 D. For direction x, y and z, these values are equal to 0.1569 D, 0.7740 D and -1.0394 D, respectively. The calculated polarizability value α_0 is equal to -137.64183 esu. The hyperpolarizability β dominated by the longitudinal components of β_{xxx} , β_{yyy} , β_{xyy} , β_{xxy} , and β_{yyz} . The large values of particular components of polarizability and hyperpolarizability indicate substantial delocalization of charges in these directions. Most of the research papers have indicated that the frontier molecular orbitals (FMO's) have

Table 6. The *Ab initio* B3LYP/cc-pVTZ (5D, 7F) calculated electric dipole moments (Debye), Dipole moments compound, polarizability (in a.u), β components and β_{tot} (10^{-30} esu) value of 2,3-diphenyl-5-(thiophen-2-ylmethylidene)-2,5-dihydro-1,2,4-triazin-6(1H)-one.

Parameters	B3LYP/cc-pVTZ	Parameters	B3LYP/cc-pVTZ
μ_x	0.1569	β_{xxx}	140.7219
μ_y	0.7740	β_{yyy}	24.0891
μ_z	-1.0394	β_{zzz}	-8.3086
μ	1.3054	β_{xyy}	-59.6642
α_{xx}	-123.1406	β_{xxy}	-23.4127
α_{yy}	-147.7063	β_{xxz}	-9.3903
α_{zz}	-142.0786	β_{xzz}	18.7507
α_{xy}	-2.2233	β_{yzz}	-22.3321
α_{xz}	0.7697	β_{yyz}	0.0588
α_{yz}	-1.8150	β_{xyy}	1.8801
$\Delta\alpha$ (esu)	-137.64183	β_{tot} (esu)	7.739×10^{-30}

significant effect on material NLO properties [63-67].

Mulliken atomic charge

The computation of the reactive atomic charges plays an important role in the application of quantum mechanical calculations for the molecular system. The Mulliken atomic charges of the title molecule were tabulated in Table 7 and shown in Fig. 6. The Mulliken atomic charges were calculated by the DFT/B3LYP method with cc-pVTZ basis set. This calculation depicts the charges of every atom in the title molecule. The magnitudes of the carbon atoms connected to hydrogen atoms were found to be generally negative value and also the carbon atoms connected to oxygen and nitrogen atoms were calculated to be negative value as expected.

Magnetic susceptibility

Atoms, molecules, free radicals or ions which contain one or more unpaired electron will possess permanent magnetic dipole moment that arises from the residual spin and angular moment of the unpaired electrons. All substances having permanent magnetic moment display paramagnetic behaviour in nature. When a paramagnetic substance is placed in a magnetic field, they will align themselves in the direction of the field and thus produces positive magnetic susceptibility, which depends on the temperature; since thermal agitation will oppose the alignment of the magnetic dipoles. The effectiveness of

diminishes increases with increase in temperature. The magnetic susceptibility (χ_m) of the molecules for various temperatures are predicted with knowledge of unpaired electron [68] and presented in Table 8. The graphical representation of ($1/\chi_m$) with T (temperature) is shown in Fig. 7. The effective magnetic moment is found to be a constant, which is 3.514×10^{-5} (BM) and Curie constant is obtained from the magnetic moment (μ_m) and is found to be 0.00083.

Nuclear magnetic resonance (NMR)

The NMR phenomenon is based on the fact that nuclei of atoms have magnetic properties that can be utilized to give chemical information. It is a research technique that exploits the magnetic properties of certain atomic nuclei. It determines physical and chemical properties of atoms or molecules. If the number of neutrons and the number of protons are both even, the nucleus has no spin. If the number of neutrons plus the number of protons is odd, then the nucleus has a half-integer spin (i.e. 1/2, 3/2, 5/2). If the number of neutrons and the number of protons are both odd, then the nucleus has an integer spin (i.e. 1, 2, and 3). The hydrogen atoms are mostly localized on periphery of the molecules and their chemical shifts would be more susceptible to intermolecular interactions as compared to that for other heavier atoms. Unsaturated carbons give signals in overlapped areas of the spectrum with chemical shift values from 100 to 200 ppm [69]. ^{13}C NMR spectra exhibit signals somewhat downfield of 170 ppm depending on the structure. Such signals are typically weak due to the absence of nuclear Overhauser effects. The external magnetic field experienced by the carbon nuclei is affected by the electronegativity of the atoms attached to them. The carbonyl carbon atom C13 in the title molecule show very downfield effect and the corresponding observed chemical shift is 168.82 ppm. The more electronegative character of the oxygen atoms renders a positive charge to the carbon and thus C1 chemical shift is observed in the more downfield shift at 159.44 ppm. The chemical shift values of other carbon atoms of the title compound are observed at 147.03, 136.82 and 134.07 ppm. The ^1H chemical shifts of the title molecule are obtained by complete analysis of their NMR spectra and interpreted critically in an attempt to quantify the possible different effects acting on the shielding constant and in turn to the chemical shift of protons. ^1H NMR spectra of the title compound indicates, the hydrogen atoms are attached with the aromatic carbons in which the peak values at 9.01, 8.19, 7.83, 7.21 and 6.72 ppm. The experimental ^1H and ^{13}C NMR chemical shifts are represented in the Fig. 8.

5. Conclusion

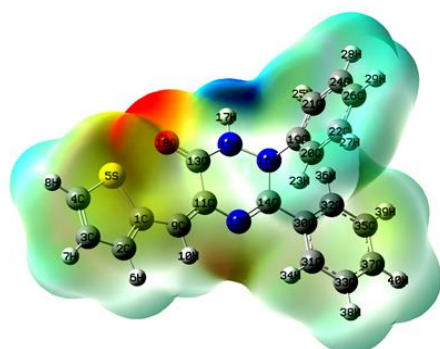


Fig. 5a. Molecular Electrostatic Potential map of 2, 3-diphenyl-5-(thiophen-2-ylmethylidene)-2, 5-dihydro-1, 2, 4-triazin-6(1H)-one.

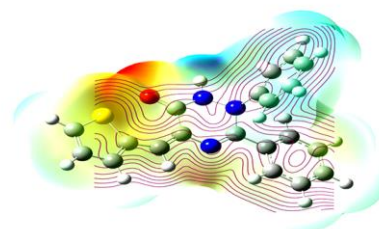


Fig. 5b. Molecular Electrostatic Potential contour map of 2, 3-diphenyl-5-(thiophen-2-ylmethylidene)-2, 5-dihydro-1, 2, 4-triazin-6(1H)-one.

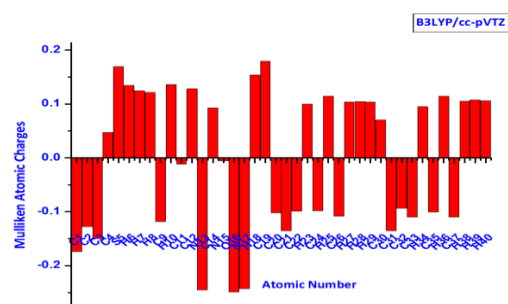


Fig. 6. Mulliken Atomic Charges of 2, 3-diphenyl-5-(thiophen-2-ylmethylidene)-2, 5-dihydro-1, 2, 4-triazin-6(1H)-one.

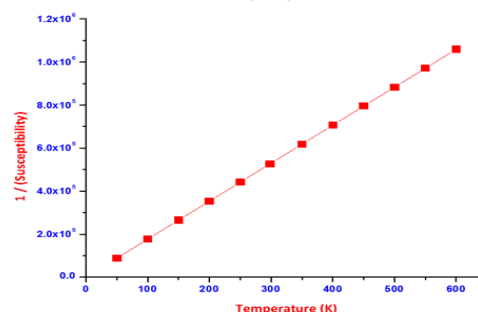


Fig. 7. Magnetic Susceptibility of 2, 3-diphenyl-5-(thiophen-2-ylmethylidene)-2, 5-dihydro-1, 2, 4-triazin-6(1H)-one.

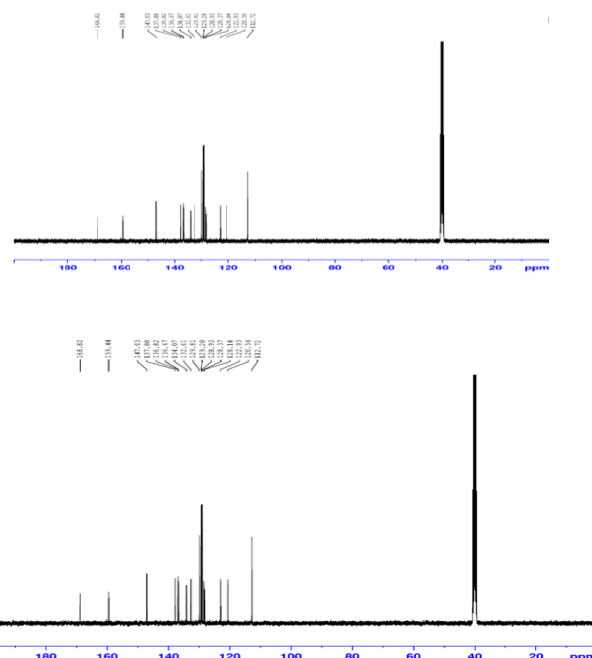


Fig. 8. ^{13}C and ^1H NMR spectra of 2, 3-diphenyl-5-(thiophen-2-ylmethylidene)-2, 5-dihydro-1, 2, 4-triazin-6(1H)-one.

Table 7. Mulliken population analysis of 2,3-d\Diphenyl-5-(thiophen-2-ylmethylidene)-2,5-dihydro-1,2,4-triazin-6(1H)-one performed at B3LYP/cc-pVTZ.

zzAtoms	Atomic Charges B3LYP/cc-pVTZ	Atoms	Atomic Charges B3LYP/cc-pVTZ
C1	-0.173753	C21	-0.13545
C2	-0.127572	C22	-0.098462
C3	-0.149615	H23	0.099709
C4	0.047176	C24	-0.097705
S5	0.169374	H25	0.114526
H6	0.134155	C26	-0.108431
H7	0.124401	H27	0.103508
H8	0.121516	H28	0.104788
C9	-0.117912	H29	0.103752
H10	0.13615	C30	0.070184
C11	-0.011716	C31	-0.134765
C12	0.127944	C32	-0.093252
N13	-0.245287	C33	-0.109552
C14	0.093139	H34	0.094887
N15	-0.005492	C35	-0.100586
O16	-0.248589	H36	0.114661
N17	-0.242846	C37	-0.109888
H18	0.153837	H38	0.105512
C19	0.179381	H39	0.107663
C20	-0.101832	H40	0.106442

Table 8. Magnetic susceptibility of 2,3-d\Diphenyl-5-(thiophen-2-ylmethylidene)-2,5-dihydro-1,2,4-triazin-6(1H)-one at various temperatures.

S. No	Temperature (K)	Susceptibility (χ_m) mole per m ³	1/ Susceptibility 1/ χ
1	50	0.000011322	88323.61774
2	100	0.000005661	176647.2355
3	150	0.000003774	264970.8532
4	200	2.8305E-06	353294.4709
5	250	2.2644E-06	441618.0887
6	298.15	1.89871E-06	526673.7326
7	350	1.61743E-06	618265.3241
8	400	1.41525E-06	706588.9419
9	450	0.000001258	794912.5596
10	500	1.1322E-06	883236.1774
11	550	1.02927E-06	971559.7951
12	600	9.435E-07	1059883.413

2,3-d\Diphenyl-5-(thiophen-2-ylmethylidene)-2,5-dihydro-1,2,4-triazin-6(1H)-one has been characterized the spectroscopic techniques such as FT-IR, FT-Raman and ¹H NMR experimentally and using the recent development of computational tool such as DFT method allow the structural analysis of the title compound conducted by B3LYP/cc-pVDZ and B3LYP/cc-pVTZ methods theoretically. The vibrational frequencies of the title compound have been precisely assigned, examined and the theoretical results were compared with the experimental results. The very good coherence has been observed between scaled wavenumbers and experimental wavenumbers. The theoretical support has been addressed by DFT calculations. NBO analysis gives the information about intermolecular and intramolecular charge transfer within the molecule. HOMO-LUMO studies reveal the intra molecular charge transfer through conjugated system. The molecular stability increased by the interaction of the electrons in a sigma bond with antibonding sigma

orbital and charge delocalization has evaluated. The molecular electrostatic potential map shows the positive potential sites are around the hydrogen atoms and the negative potential sites are on electronegative atoms. ¹H and ¹³C NMR chemical shifts are experimentally analyzed. Above said sites give details about the region where the compound can have intermolecular interactions. This work will be very useful for the design and synthesis new materials.

Reference:

- [1] B. Giovanna, M. Manuela, S. Giovanna. The versatile thiophene: An overview of recent research on thiophene-based materials. 17 (13): (2005)1581-1593.
- [2] A. A. Patel, G. A. Mehta; Der Pharma Chemica; 2(1); (2010) 215-223.
- [3] W. Meyer, Ber. Dtschn. Chem. Ges.; 16 (1883) 1465-1478.
- [4] J. A. Joule, G. F. Smith; In: Van Norstrand Reinhold; Heterocyclic Chemistry; London; (1972).
- [5] Y.Z. Su, J.T. Lin, Y.T. Tao, C.W. Ko, S.C. Lin, S.S. Sun Chem Mater 14 (2002) 1884-1890.
- [6] T. Osaka, S. Komaba, K. Fujihana, N. Okamoto, T. Momma, N. Kaneko Electrochem Soc 144(2) (1997) 742-448.
- [7] J. L. Reddinger, J. R. Reynolds, Advances in Polymer Science, 145 (1999) 57122-57135.
- [8] D. T. McQuade, A. E. Pullen, T.M. Swager, Chemical Reviews, 100 (2000) 2537-2574.
- [9] I. C. Choong, W. Lew, D. Lee, P. Pham, M.T. Burdett, J. W. Laam, C. Wiesmann, T. N., Luong, B. Fahr, W.L. DeLano, R. S. McDowell, D. A. Allen, D. Erlanson, E.M. Gordon, T. , O'Brien T, J. Med Chem, 45 (2002) 5005-5022.
- [10] K. Dore, S. Dubus, H.A. Ho, I. Levesque, M. Brunette, G. Corbeil, M. Boissinot, G., Boivin, M. G. Bergeron, D. Boudreau, M. Leclerc, Journal of the American Chemical Society, 126 (2004) 4240-4244.
- [11] Merck Index, 13th Edition, Merck & Co, Inc, Whitehouse Station, New Jersey, (2001).
- [12] J. Bakker, F.J. Gommers, I. Nieuwenhuis, H. Wynberg, Journal of Biological Chemistry, 254 (1979) 1841-1844.
- [13] S. Iyengar, J.T. Arnason, B.J.R. Philogene, P. Morand, N.H. Werstiuk, G. Timmins, Pesticide Biochemistry and Physiology, 29 (1987) 1-9.
- [14] J. Daisy Magdaline, T. Chithambarathanu, Journal of Applied Chemistry, 8 (2015) 06-14.
- [15] X.H. Li, X.R. Liu, X.Z. Zhang Comput Theor Chem 969 (1-3) (2011) 27-34.
- [16] L.L. Lu, H. Hu, H. Hou, B.S. Wang, Comput. Theor. Chem. 1015 (2013) 64-71.
- [17] T. Yanai, D.P. Tew, N.C. Handy (CAM-B3LYP) Chem Phys Lett 393(1-3) (2004) 51-57.
- [18] N.C. Handy, P.E. Maslen, R.D. Amos, J.S. Andrews, C.W. Murry & G. Laming, Chem. Phys Lett, 197 (1992) 506-511.
- [19] N.C. Handy, C.W. Murry & R.D. Amos, J Phys Chem, 97 (1993) 4392-4396.
- [20] P.J. Stephens, F.J. Delvin, C.F. Chavalowski & M. Frish, J Phys Chem, 99 (1995) 16883-16902.
- [21] M.J. Frisch, G.W. Trucks, H.B. Schlegel, G.E. Scuseria, M.A. Robb, J.R. Cheeseman, G. Scalmani, V. Barone, G.A. Petersson, H. Nakatsuji, M. Caricato, X. Li, H.P. Hratchian, M. Hada, A.F. Izmaylov, J. Bloino, G. Zheng, J.L. Sonnenberg, M. Ehara, K. Toyota, R. Fukuda, J. Hasegawa, M. Ishida, T. Nakajima, Y. Honda, O.

- Kitao, H. Nakai, T. Vreven, J.A. Montgomery, F. Ogliaro, M. Bearpark, J.J. Heyd, E. Brothers, K.N. Kudin, V.N. Staroverov, R. Kobayashi, J. Narmond, K. Raghavachari, A. Rendell, J.C. Burant, S.S. Iyengar, J. Tomasi, M. Cossi, N. Rega, J.M. Millam, M. Klene, J.E. Knox, J.B. Cross, V. Bakken, C. Adamo, J. Jaramillo, R. Gomperts, R.E. Stratmann, O. Yazyev, A.J. Austin, R. Cammi, C.Pomelli, J.W. Ochterski, R.L. Martin, K. Morokuma, V. G. Zakrzewski, G. A. Voth, P. Salvador, J.J. Dannenberg, S. Dapprich, A.D. Daniels, O. Farkas. J. B. Forseman, J.V. Ortiz, J. Cioslowski, D.J. Fox, Gaussian 09, Revision B.01. Gaussian, Inc, Wallingford CT (2009).
- [22] M. Oftadeh, S. Naseh, M. Hamadani, Computational and Theoretical Chemistry, 966 (2011) 20-25.
- [23] K. Sadasivam, R. Kumaresan, Computational and Theoretical Chemistry, 963 (2011) 227- 235.
- [24] A. H. Raheem, H. M. Abduljalil, T. A. Hussein, Journal of KUFA – Physics, 5 (2013) 46- 52.
- [25] J.S. Kwiatkowski, J. Leszczynski, I. Teca, J. Mol. Struct. 436-437 (1997) 451-480.
- [26] B. Bak, D. Christensen, L. Hansen-Nygaard, J. Rastrup-Andersen, J. Mol. Spectrosc. 7(1961) 58-63.
- [27] T. Gupta, R. Wrzalik, G. Pasterna, K. Pasterny, J. Mol. Struct. 616 (2002) 17-32.
- [28] P.J. Trotter, Applied Spectroscopy, 31 (1977) 30-35.
- [29] L.J. Bellamy, The Infrared Spectra of Complex Molecules, Chapman and Hall, London, (1975).
- [30] Y.R. Sharma, Elementary organic spectroscopy — principles and chemical applications, S. Chand and Company Ltd., New Delhi, (1994).
- [31] G. Socrates, Infrared Characteristic Group Frequencies, Wiley Interscience Publication, (1980).
- [32] G. Varsanyi, Vibrational Spectra of Benzene Derivatives, Academic press, New York, (1969).
- [33] N. Prabavathi, V. Krishnakumar, Spectrochim Acta A, Mol. Biomol. Spectrosc. 72 (2009) 743–747.
- [34] A. Altun, K. Golcuk, M. Kumru, J Mol Struct (Theochem) 637 (2003) 155–639.
- [35] N.B. Colthup, L.H. Daly, S.E. Wiberley, Introduction to infrared and Raman Spectroscopy, Academic Press, New York, (1990).
- [36] G. Socrates, Infrared Characteristic Group Frequencies, Wiley Interscience Publication, New York, (1980).
- [37] L.M. Sverdlov, M.A. Kovner, E.P. Krainnov, Vibrational Spectra of Poly Atomic Molecules, Nauka, Moscow, (1970).
- [38] Y. Atalay, D. Avci, A. Basoglu, Structural Chemistry, 19 (2008) 239 -249.
- [39] M. Kurt, P. C. Babu, N. Sundaraganesan, M. Cinar, M. Karabacak, Spectrochimica Acta Part A 79 (2011) 1162–1170.
- [40] K. Chaitanya, Spectrochim. Acta A 86 (2012) 159-173.
- [41] E. Kavitha, N. Sundaraganesan, S. Sebastian, Indian J. Pure Appl. Phys. 48 (2010) 20-30.
- [42] A. Jayaprakash, V. Arjunan, S. Mohan, Spectrochim. Acta A 81 (2011) 620-630.
- [43] R.G. Parr, W. Yang, Functional Theory of Atoms and Molecules, Oxford University Press, New York, (1989).
- [44] P.W. Ayers, R.G. Parr, J. Am. Chem. Soc. 122 (2000) 2010-2018.
- [45] R. G. Parr, W.J. Yang, Am. Chem. Soc. 106 (1984) 511-513.
- [46] P.K. Chattaraj, B. Maiti, U. Sarkar, J. Phys. Chem, A 107 (2003) 4973-4975.
- [47] C. Morell, A. Grand, A. Toro-Labbe, J. Phys. Chem. A 109 (2005) 205-212
- [48] A.E. Reed, L. A. Curtiss, F. Weinhold, Chemical Reviews, 88 (1988) 899-926.
- [49] C. James, A. Amal Raj, R. Reghunathan, I.H. Joe, V.S. Jayakumar, J. Raman Spectrosc. 37 (2006) 1381-1392
- [50] J. Liu, Z. Chen, S. Yuan, J. Zhejiang, Univ. Sci. B6, (2005) 584-589.
- [51] P. Rubarani, S. Gangadharanand, Sampath Krishnan, Acta Physica Polonica A, 125 (2014) 18-22.
- [52] P. Agarwal, S. Bee, A. Gupta, P. Tandon, V.K. Rastogi, S. Mishra, Spectrochim. Acta A. 121 (2014) 464-482.
- [53] A. Tokath, E.Ozen, F. Uzun, S. Bahceli, Spectrochim. Acta A, 78 (2011) 1201-1211.
- [54] E. Scrocco, J. Tomasi, Adv. Quantum Chem. 11 (1979) 115-121.
- [55] F.J. Luque, J.M. Lopez, M. Orozco, Theoret. Chem. Acc. 103 (2000) 343 – 345.
- [56] N. Okulik, A.H. Jubert, int. Electron J. Mol. Des, 4 (2005) 17-30.
- [57] P.N. Prasad, D.J. Williams, Introduction to Non-linear optical effects in Molecules and Polymers, John Wiley & Sons, New York (1991).
- [58] F. Kajzar, K.S. Lee, A.K.Y. Jen, Adv. Polym. Sci-161 (2003) 1-5.
- [59] V. Krishnakumar, R. Nagalakshmi. Physica B 403 (2008) 1863-1869.
- [60] V. Jerald Ramaclus, Tina Thomas, S. Ramesh, P. Sagayaraj, E.A. Michael, Cryst. Eng. Comm. 16 (2014) 6889-6895.
- [61] N. Sundaraganesan, E. Kavitha, S. Sebastian, J.P. Cornard, M. Martel, Spectrochimica Acta A, 74 (2009) 788-797.
- [62] H. Alyar, Z. Kantarci, M. Bahat, E. Kasap. J. Mol. Struct. 834-836 (2007) 516-520.
- [63] R. Zhang, B. Du, G. Sun, Y.X. Sun, Spectrochim. Acta A 75 (2010) 1115-1124.
- [64] D.W.Y.L. Fei-Fei Li, Polymer 47 (2006) 1749-1754.
- [65] K. Oberg, A. Berglund, U. Edlund, B.J. Eliasson, Chem. Inf. Comput. Sci. 41 (2001) 811 814.
- [66] W. Zheng, N.B. Wong, W.K. Li, A. Tian, Journal of Chemical Theory and Computation. 2 (2006) 808-814.
- [67] Tuncay Karakurt, Muharrem Dincer, Alaaddin Cukurovali, Journal of Molecular Structure, 991 (2011) 186-201.
- [68] M.C. Gupta, Atomic and Molecular Spectroscopy, New Age International Private Limited Publishers, New Delhi, (2001).
- [69] R.M. Silverstein, F.X. Webster, Spectrometric Identification of Organic Compounds, sixth ed., John Wiley & Sons, Chichester, (2004).